

Probing the Schottky barrier with conduction electron spin resonance

J. M. Anderberg, G. T. Einevoll,* D. C. Vier, S. Schultz, and L. J. Sham
Department of Physics, University of California, San Diego, La Jolla, California 92093-0319
 (Received 22 April 1996; revised manuscript received 4 February 1997)

The Schottky barrier of a heavily doped Si layer covered with a metal film is investigated using conduction electron spin resonance, which is utilized *in situ* in UHV to continuously monitor the metal overlayer development from a fractional monolayer through multiple layers. Measured increases in linewidth are compared with calculations based on a kinetic theory. For Al and Ag, the data can be explained both by flat-surface and island models, even though for Al only a flat-surface model with smooth surfaces is compatible with the experiments. In contrast, for Cu and Al-Cu bilayers, the data unambiguously favor the rough-surface island model. [S0163-1829(97)05320-4]

I. INTRODUCTION

We report a detailed¹ study of the Schottky barrier using conduction electron spin resonance (CESR).²⁻⁵ CESR studies of electron transport across the metal semiconductor interface complement other techniques that probe the Schottky barrier such as I-V, capacitance, ballistic electron emission spectroscopy (BEEM),⁶ etc., but CESR is uniquely useful because it is applicable to varying dopant levels from the regime of a Schottky barrier to the formation of an Ohmic contact, and because it provides information from fractional through multimonomer metal coverages. Moreover, it measures the spin transport across an interface, which may be relevant in developing spin-related devices⁷ and optoelectronic processes.⁸ Previous CESR studies of electron spin transport across an interface include bilayers of two metals^{9,10} and a metal film covered with fractional monolayers of a second, nonmagnetic,¹¹ or magnetic¹² material. In this paper we study silicon heavily doped with phosphorus and covered with Cu, Ag, or Al.

We measure the change in the linewidth of the CESR absorption signal in a specially prepared thin phosphorus-doped Si (Si:P) layer when additional spin relaxation channels are introduced following evaporation of a metal onto the free Si surface. Conduction electrons in Si, which diffuse toward and subsequently impact on the metal, may undergo spin relaxation via two general processes: (1) impact followed by reflection (either specular or diffuse) or (2) impact resulting in tunneling across the interface. For those electrons that do tunnel across the interface, there are five subsequent spin relaxation opportunities before returning to the Si: (i) during the tunneling process, (ii) scattering from impurities in the bulk metal, (iii) reflection from the metal free surface, (iv) reflection at the Si-metal interface when impacting from the metal side, and (v) when tunneling back into the semiconductor. All these processes are not independent, and the general spin transport, including the tunneling probabilities across the interface, may be characterized by a minimum independent set of parameters after taking into account charge conservation and detailed balance conditions (cf. Ref. 9).

A theoretical study is made of the spin disorientation probability. These spin relaxation processes depend on (i) whether the metal film is flat or consists of islands and (ii) whether the reflections off the metal surface and metal-Si

interface are specular (smooth interfaces) or diffuse (rough interfaces). The theoretical results from the different interface models are sufficiently distinct that experimental data can be seen as favoring the island scenario. The combination of experiment and theory provides a tool for studying the effects of the Schottky barrier on the electrons transporting charge and spin across the interface.

II. EXPERIMENTAL DETAILS

The Si:P samples consist of a thin region, ~ 200 Å thick, heavily *n* doped with phosphorus ($n_p = 3 \times 10^{20}$ cm⁻³) located at the Si surface and a much thicker, less heavily doped region ($n_p < 5 \times 10^{19}$ cm⁻³) extending from the heavily doped region to a depth of ~ 3 μm. The thin, heavily doped region has a very high concentration to ensure that, when a metal layer is deposited on the Si:P surface, the Schottky barrier is narrow enough to allow sufficient tunneling into the metal. The other, much thicker, doped region is included in order to provide a large source of conduction electrons to assure a sufficiently strong CESR signal. The dopant profile of the less heavily doped region was characterized by sheet-resistance measurements on a test substrate and was found to be roughly Gaussian, i.e.,

$$n_p(x) \approx 5 \times 10^{19} \text{ cm}^{-3} e^{-(x/1.18 \text{ } \mu\text{m})^2}$$

for $0.02 \text{ } \mu\text{m} < x < 3 \text{ } \mu\text{m}$. (1)

The Si:P samples were prepared for the UHV system by the following standard procedure. First they were cleaned for 10 min in a 5:1:1 solution of H₂O:H₂O₂:NH₄OH heated to 70 ± 5 °C. After rinsing in deionized water they were further cleaned for 10 min in an 8:2:1 solution of H₂O:H₂O₂:HCl also heated to 70 ± 5 °C. Following another rinse in deionized water, the samples were dipped in a dilute solution of HF to remove the thin oxide layer built up during cleaning and to hydrogen passivate the Si:P surface. This hydrogen passivation inhibits future oxide growth.

We have measured the C, O, and SiO₂ Auger peaks of samples that were exposed to air for different periods of time after following the above preparation procedure. We found

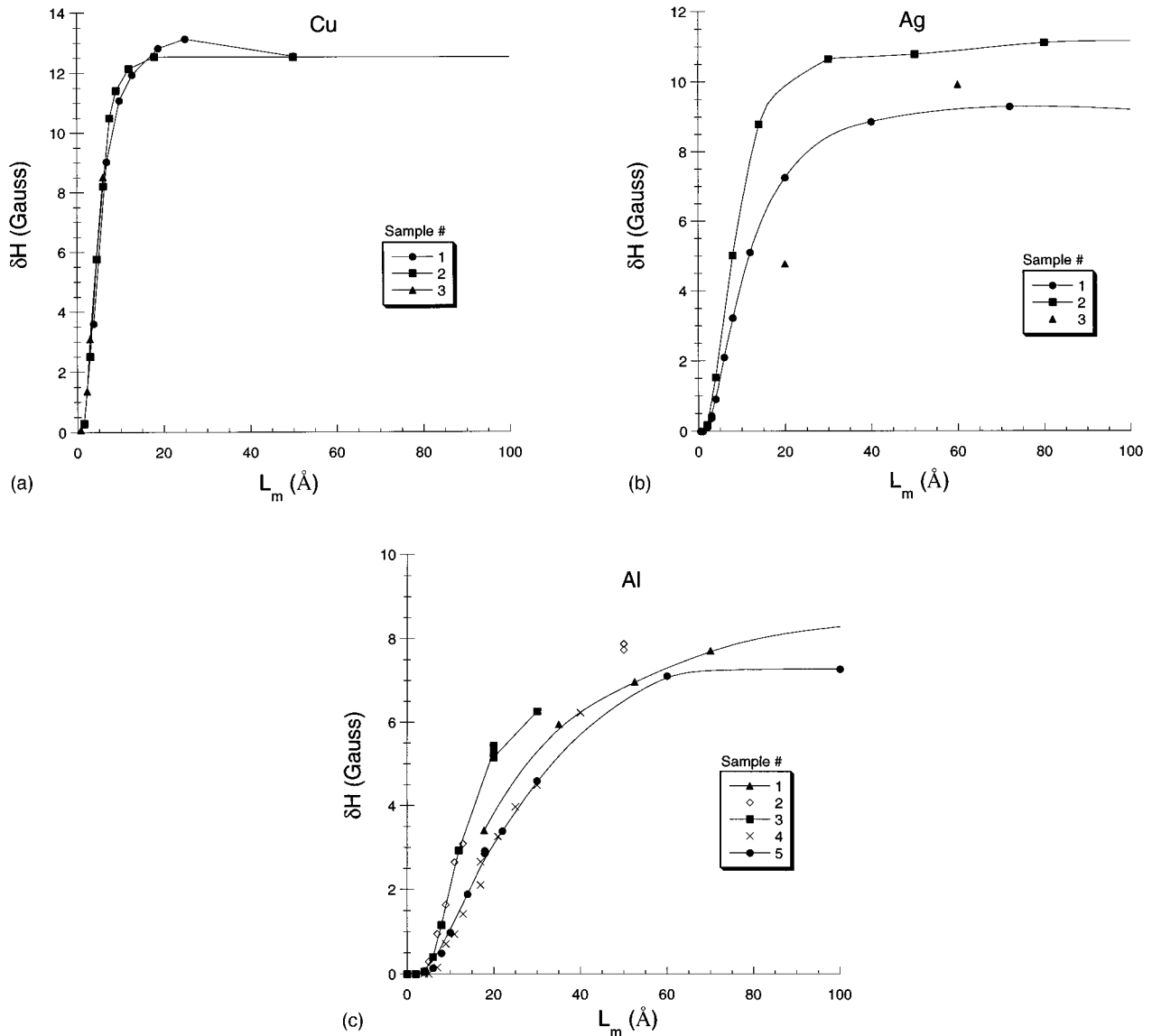


FIG. 1. Change in CCSR absorption linewidth δH for typical Si:P samples measured as a function of thickness L_m for deposited Cu, Ag, and Al.

that after an hour of air exposure the surface oxidation and carbon contamination was typically a monolayer or less. The typical time to load a sample into the UHV chamber after the HF dip is only about 4 min, and the load lock pressure reaches 10^{-5} Torr within 15 min.

We note that *in situ* heat treatments of the Si:P samples were attempted in order to provide cleaner surfaces before metal deposition. However, the heat treatment was found to be impractical, as it severely depleted the phosphorus dopant concentration near the sample surface at the temperatures required to remove oxygen and carbon contamination.

The metal (Cu, Ag, or Al) was evaporated from an MBE oven onto the Si:P (111) substrate at room temperature. The evaporation pressure was typically less than 10^{-7} Torr. The mass-averaged metal film thickness L_m was measured using a quartz crystal microbalance. The stability of the system was such that the deposition was done in increments as small as 0.1 mass-equivalent monolayer. (Note that all experimental thicknesses are averaged-mass equivalents). After metal evaporation the sample was transported *in situ* to a TE₁₀₂

cavity where the CCSR absorption line was measured after cooling the sample to a temperature of 77 K. During the CCSR measurements the sample was always under UHV ($\sim 10^{-10}$ Torr) conditions. A detailed description of the UHV apparatus with *in situ* sample preparation and CCSR capability may be found in the thesis of Anderberg.¹³

III. EXPERIMENTAL DATA

The change in the Si:P CCSR linewidth (δH) was studied as a function of metal layer thickness, from submonolayer coverages up to film thicknesses of 200 Å (Fig. 1). While a good reproducibility of data was observed for Cu, the Ag and Al data showed more scatter. For all cases the linewidth showed no further increase for thicknesses greater than 60 Å. Note that each curve shows a threshold thickness before any linewidth increase is observed, followed by a relatively rapid increase, then a plateau at a final value. A summary of representative experimental data for each metal for L_m less than 60 Å is shown in Fig. 2. Important qualitative features are

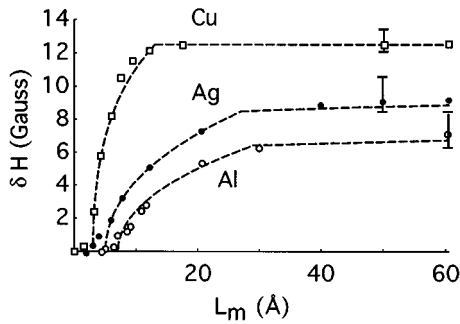


FIG. 2. Comparison of theory with measured changes in CCSR absorption linewidth δH for typical Si:P samples measured as a function of thickness L_m for deposited Cu (\square), Ag (\bullet), or Al (\circ). The dashed lines are theoretical results using $D=9.5 \times 10^{-4} \text{ m}^2/\text{s}$, $v_{Fs}=1.8 \times 10^5 \text{ m/s}$, and $L=1 \mu\text{m}$ assuming rough surfaces and islands. The calculation is normalized to match the experimental value of δH at $L_m=100 \text{ \AA}$. The other parameters are $h_0=10, 22, \text{ and } 22 \text{ \AA}$ and $L_{on}=3, 5, \text{ and } 7 \text{ \AA}$ for Cu, Ag, and Al, respectively. The error bars shown indicate the range of plateau values of δH for multiple samples.

that (i) the width of the CCSR resonance peak increases from $\sim 10 \text{ G}$ for the initial Si sample to $15\text{--}25 \text{ G}$ for the Si-metal system in the bulk saturation limit, (ii) the bulk limit typically occurs for metal thicknesses of a few tens of angstroms, $L_m=15 \text{ \AA}$ for Cu and $L_m \sim 50 \text{ \AA}$ for Ag and Al, and (iii) the sharp onset for broadening does not occur until a mass-averaged metal thickness L_m reaches the onset thickness $L_{on}=3, 5, \text{ and } 7 \text{ \AA}$ for Cu, Ag, and Al, respectively.

To give further insight into the evolution of the Schottky barrier, the CCSR linewidth was also studied with metal bilayers on the Si:P surface. In these experiments a metal is evaporated on the Si:P surface to a given thickness, resulting in an increase of the CCSR linewidth. A second metal is subsequently deposited over the first and the CCSR linewidth monitored as a function of the thickness of the second metal. We studied both Cu-Ag and Al-Cu bilayers on the Si:P surface.

Figure 3 shows the results for Cu-Ag bilayers on three Si:P samples. The samples had an initial layer of Cu evaporated on them, with thicknesses of $3, 6, \text{ and } 9 \text{ \AA}$, respectively. This was followed by 3 \AA of Ag on each sample (marked by arrows in Fig. 3), then capped with Ag for a total bilayer metal thickness of 50 \AA . Note that the Cu-Ag curves closely follow the pure typical Cu curve, indicating that the Cu interface is already defined with only 3 \AA of Cu on the Si:P surface.

Figure 4 shows the results for Al-Cu bilayers on three Si:P samples. Al is first evaporated to a selected thickness (and δH is measured), followed by successive depositions of Cu. When an initial 10 \AA of Al deposit is covered with Cu (curve A), δH rises rapidly, similar to that of pure Cu samples (represented by the shaded region). With 20 \AA of initial Al (curve B) there is a less rapid rise, but as with 10 \AA of Al the plateau value of δH is essentially that of pure Cu. In contrast, when 60 \AA Al is covered with Cu (curve C) δH simply approaches the pure Al bulk value. This suggests, by means of the island model in Sec. V B, that for initial layers thinner than a few tens of angstroms, Al islands may form and only partially cover the Si surface, so that consecu-

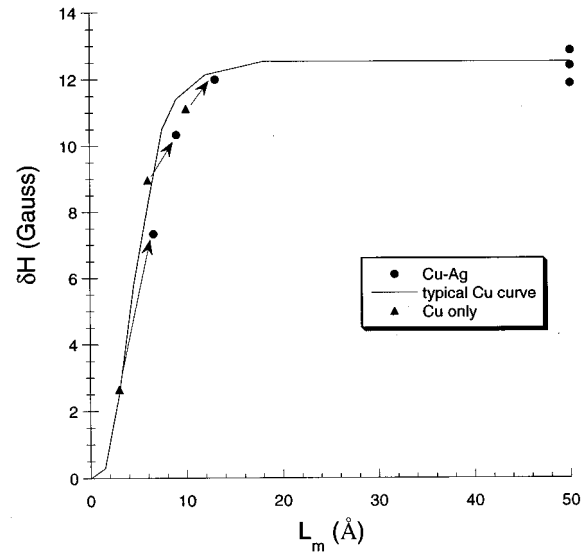


FIG. 3. Change of CCSR linewidth for three samples of Cu-Ag bilayers on Si:P. L_m is the total metal thickness. The initial Cu thickness is $3, 6, \text{ and } 9 \text{ \AA}$, respectively, for the three samples, shown as the beginning of an arrow. The first deposit of Ag on each sample increases the total thickness by 3 \AA and results in a linewidth increase shown at the tip of an arrow. After the second Ag deposition, the total metal thickness is 50 \AA for each sample.

tively added Cu penetrates to the Si slab and ends up defining the Schottky barrier. An initial 60-\AA Al layer, on the other hand, is sufficient to protect the Al-Si interface from the added Cu.

IV. THEORY OF CCSR LINEWIDTH

In our theory we calculate the increased CCSR width by considering the metal layer as a source of spin scattering for a conduction electron in the Si slab colliding with the metal-semiconductor interface. There is a small net spin polarization due to the Pauli susceptibility in the applied magnetic field for resonance $\sim 3 \text{ kG}$. The probability for electrons at

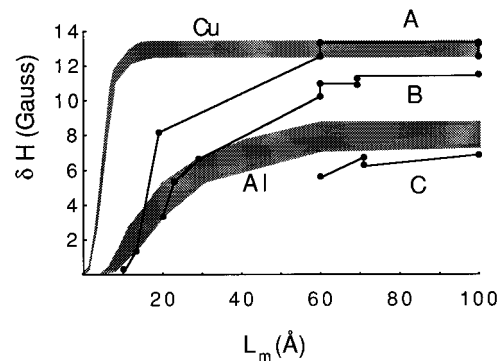


FIG. 4. Change of CCSR linewidth for an initial film of Al deposited on Si followed by successive Cu depositions. L_m is the total metal thickness. The initial Al thickness is $10, 20, \text{ and } 60 \text{ \AA}$ for curves A, B, and C, respectively. The steps in the solid curves are changes after waiting periods of the order of one day. The shaded regions cover the various samples for pure Cu and pure Al. Due to sample variations, the initial δH of the solid curves does not always lie within the pure Al region.

the Fermi surface to tunnel into the metal depends on the nature of the Schottky barrier and the angle of incidence. These electrons eventually return to the Si slab with or without having suffered a spin-scattering collision in the metal layer. When the time of the electron residing in the metal is short, this can be viewed as spin-polarized electrons in the Si slab scattering off the metal-semiconductor interface with a probability ϵ for spin disorientation in the process. We thus need a theory that (i) relates ϵ to the increase in the CESR absorption peak width, and (ii) gives the dependence of ϵ on the metal film thickness. Clearly, the spin-flip rate depends on the structure of the interface through which the electrons pass. We study the consequences for (i) flat metal surfaces and metal films consisting of islands and (ii) specular and diffuse electron reflections in the metal film.

A. Linewidth in terms of spin disorientation

For a Si:P slab of thickness L where the conduction electrons have a probability ϵ for suffering a spin-disorienting collision at the interface once the metal is added, the increase, $\delta'H$, of the peak-to-peak width, ΔH , of the derivative of the resonance signal due to surface scattering, assuming a Lorentzian signal, is¹⁴

$$\delta'H = \frac{1}{2\sqrt{3}} \frac{1}{\gamma} \frac{\epsilon v_{F_s}}{L(1 + \epsilon v_{F_s} L / 8D)}, \quad (2)$$

where v_{F_s} is the Fermi velocity, D is the isotropic diffusion coefficient, and γ is the gyromagnetic constant of the electron in Si. The prime in $\delta'H$ is used to distinguish it from $\delta H = \Delta H(L_m) - \Delta H(L_m=0)$, the increment of linewidth from zero to finite metal layer thickness, which the experiments record (cf. Fig. 1) and which, for comparison, the theory calculates as $\delta H = \delta'H(L_m) - \delta'H(L_m=0)$. $\Delta H(L_m)$ can be related to the transverse spin-relaxation time T_2 , which is in turn equal to the spin-lattice relaxation time T_1 for cubic materials.

B. Theory of spin disorientation probability

1. Model of flat interface

To find the spin-disorientation probability ϵ , we first consider an ideal metal film, with both surfaces smooth, providing specular reflections for the electron. Then, ϵ is determined by the probability of the electron tunneling from Si into the metal layer and *not* returning with the same spin direction,

$$\epsilon = \bar{T} \left[1 - \int_0^\infty dt \omega_t(t) P(t) \right], \quad (3)$$

where $\bar{T} = \langle v_\perp T \rangle / \langle v_\perp \rangle$ is the tunneling probability into the metal averaged over the Si Fermi surface, and $\omega_t(t)$ is the rate at time t for tunneling back from the metal to Si. The probability $P(t)$ for the initially spin-polarized electron to remain polarized and to remain in the metal after time t is governed by the rate equation

$$\frac{dP}{dt} = -[\omega_t(t) + \omega_s]P, \quad P(0) = 1, \quad (4)$$

where ω_s is the total spin-disorienting collision rate, consisting of a bulk term due to spin scattering in the bulk metal, estimated from CESR data¹⁵ and two surface terms due to spin flips at the free metal surface and at the metal-Si interface.

The time dependence of the tunneling rate from the metal back to the semiconductor arises from the momentum scatterings suffered by the electron in the metal region. We make a simple model of the time dependence as follows. *Before* the spin-polarized electron in the metal suffers a momentum collision, the probability for tunneling back into the Si slab is just \bar{T} and the tunneling rate back is \bar{T} times the frequency of hitting the metal-Si interface, i.e., for $t < \tau$, the (Drude) momentum-relaxation time,¹⁶ $\omega_t(t) \equiv \omega_t = \bar{T} v_{F_m} / (4L_m)$. The factor of 4 comes from the traversal time across the thickness L_m and back at the average speed normal to the surface, which is half the Fermi speed v_{F_m} in the metal. *After* the spin-polarized electron suffers a momentum collision, it is assumed to have an equal probability to be anywhere on the metal Fermi surface. Then, for $t > \tau$, the principle of detailed balance across the Si-metal interface yields the return tunneling rate, $\omega_t(t) = f \omega_t(t < \tau)$, where $f = 6(k_{F_s}/k_{F_m})^2$, the Fermi radius k_{F_s} of Si being much smaller than that of the metal k_{F_m} .

From Eqs. (3) and (4) one then obtains the disorientation probability

$$\epsilon = \bar{T} \left[\frac{\omega_s}{\omega_t + \omega_s} + \left(\frac{\omega_t}{\omega_t + \omega_s} - \frac{f \omega_t}{f \omega_t + \omega_s} \right) e^{-(\omega_t + \omega_s)\tau} \right]. \quad (5)$$

The terms in this expression can be understood as follows. The overall factor of the tunneling probability signifies tunneling being the prime driving mechanism for the loss of spin information. Of course, there would be no loss of spin information should all the electrons then return to the semiconductor without suffering any spin-disorienting collisions. The first factor inside the square brackets is the fraction of the electrons returning to the semiconductor region with disoriented spin when *no* momentum-scattering collisions occur. The second term in the brackets represents the difference made to the spin loss of the returned electrons due to momentum scattering in the metal.

To obtain the thickness dependence explicitly we use

$$\omega_s = \omega_b + v_{F_m} \eta / (4L_m), \quad (6)$$

where ω_b is the bulk spin-disorientation rate in the metal, η is the sum of the spin-disorientation probability at the free metal surface and at the metal-Si interface, and $4L_m/v_{F_m}$ is the traversal time across the metal layer and back, as described above. To make the competing physical causes obvious, we introduce the spin scattering length $\Lambda = v_{F_m}/4\omega_b$ in the metal layer. Then

$$\begin{aligned} \epsilon(L_m) = & \bar{T} \frac{\eta + L_m/\Lambda}{\bar{T} + \eta + L_m/\Lambda} \\ & \times \left(1 + \frac{(1-f)\bar{T}}{f\bar{T} + \eta + L_m/\Lambda} e^{-\omega_b \tau (\Lambda/L_m) (\bar{T} + \eta + L_m/\Lambda)} \right). \end{aligned} \quad (7)$$

The physical origins of the terms are \bar{T} from tunneling, η from the interface and surface spin scatterings, and L_m/Λ

from the bulk spin scattering proportional to the metal layer thickness L_m in units of the spin scattering length. The factor f is a measure of the detailed balance between the metal and the semiconductor. In the present study the spin scattering rate in the metals is much lower than the momentum scattering rate, i.e., $\omega_b \tau \ll 1$. Note that $\omega_b \tau \Lambda = \tau v_{Fm}/4$ is the mean free path. The mean-free path limited tunneling or surface spin scattering $\omega_b \tau \Lambda (\bar{T} + \eta)$ competes with the thickness L_m in the exponent. When the thickness is increased to the regime $L_m/\Lambda \gg \omega_b \tau (\bar{T} + \eta)$, Eq. (7) simplifies to

$$\epsilon(L_m) = \bar{T} \frac{\eta + L_m/\Lambda}{f\bar{T} + \eta + L_m/\Lambda}. \quad (8)$$

It is then readily seen that the spin disorientation probability has two plateaus as the metal layer thickness increases:

$$\epsilon(L_m) \sim \bar{T} \eta / (f\bar{T} + \eta) \quad \text{when } L_m/\Lambda \ll \eta, \quad (9)$$

$$\epsilon(L_m) \sim \bar{T} \quad \text{when } L_m/\Lambda \gg f\bar{T} + \eta. \quad (10)$$

The rise between the first [Eq. (9)] and second [Eq. (10)] plateaus comes from the competition between the bulk spin scattering in the metal versus tunneling and surface scattering. The second plateau demonstrates that spin information in the semiconductor is lost via electron tunneling through the Schottky barrier. Since f is small, the first plateau is almost at the same height as the second.

The formula for $\epsilon(L_m)$ in Eq. (7) is derived for specular reflections (smooth interfaces). For diffuse scattering (rough interfaces) we take it to mean that any reflection would randomize the electron momentum. This is equivalent to putting $\tau = 0$ in Eqs. (5) and (7), which means that Eq. (8) is applicable for *all* film thicknesses L_m in the diffuse scattering case. Thus, in the case of diffuse scattering, a transition in $\epsilon(L_m)$ from the small thickness value $\eta/(f\bar{T} + \eta)$ to the large thickness value \bar{T} occurs for $L_m \sim \Lambda(f\bar{T} + \eta)$.

The transmission probability T is evaluated using (i) the standard expressions for the Schottky barrier and the depletion width,¹⁷ (ii) an isotropic effective mass $m_s = 0.45m_0$ (m_0 being the free-electron mass) for the electron in the more heavily doped Si, (iii) the free-electron model for the metal, and (iv) the boundary conditions at the metal-semiconductor interface,¹⁸

$$\psi_s = \psi_m, \quad (11)$$

$$\psi'_s / (2m_s) = \psi'_m / m_0 \quad (12)$$

for the envelope function ψ_s in Si and the metal wave function ψ_m and their slopes at the boundary. Note the factor of 1/2 in the matching of the slopes in the second equation. It comes from the Bloch wave nature in the semiconductor versus the simple plane-wave approximation of the electron in the metal.¹⁸

2. Island model for the interface

From the measured variation of δH with the thickness of the adsorbed metal layer at the initial stage (Fig. 2), we infer that an onset distance L_{on} exists for the ultrathin film in which the bulklike metal has not yet been established and that growth of three-dimensional islands occurs after the for-

mation of the the onset layer. We also assume that the Si electrons do not significantly spin scatter off the deposited metal atoms, which is supported by estimates with adsorbed atoms on metal surfaces.¹⁹ Guided by the structural studies of adsorption of Ag on a Si(111) surface,²⁰ we construct an empirical formula for the island height $h(L_m)$ given by

$$h(L_m) = \sqrt{(L_m - L_{on})h_0} \quad \text{for } L_{on} < L_m < L_{on} + h_0, \quad (13)$$

i.e., a square-root dependence on the average thickness (minus the onset) to a maximum growth of height h_0 that depends on the specific metal. We assume that the electron tunneling into an island is not affected by the side walls, which should be valid if the lateral dimension of the island is larger than the Si Fermi wavelength, i.e., about 10 Å. By the definition of the mass-averaged metal layer thickness L_m , the mass of the uniform layer of thickness $L_m - L_{on}$ covering the whole Si sample surface is the same as the islands of height $h(L_m)$, which, therefore, must occupy the fraction of the surface $(L_m - L_{on})/h(L_m)$. Then the effective surface-scattering probability is found for the islands (when $L_{on} < L_m < L_{on} + h_0$) within our model to be

$$\bar{\epsilon} = \sqrt{(L_m - L_{on})/h_0} \epsilon(\sqrt{(L_m - L_{on})h_0} + L_{on}), \quad (14)$$

where we are taking the area with metal thickness L_{on} to have no spin scattering and the area with metal thickness of the island plus the onset layer to have the same spin disorientation probability as a uniform layer of the same thickness. After the islands are filled ($L_m > L_{on} + h_0$), the spin disorientation probability returns to

$$\bar{\epsilon} = \epsilon(L_m). \quad (15)$$

Thus when metal islands are present the observed thickness dependence of ϵ will result from a convolution of the thickness dependence of the island structure and the (flat-surface) spin-disorientation formula $\epsilon(L_m)$ in Eq. (7).

V. APPLICATION OF THEORY TO MEASURED SYSTEMS

A. Flat surfaces

We model the Si:P sample with varying phosphorus-doping concentration as a two-slab system with a thin layer ($L = 200$ Å, $n_p = 3 \times 10^{20}$ cm⁻³, $m_s = 0.45m_0$) next to the metal forming part of the Schottky barrier, and a second layer of uniform doping concentration ($L \sim 1$ μm, $n_p = 5 \times 10^{19}$ cm⁻³, $m_s = 0.41m_0$) representing Si in the less heavily doped region in which CESR is observed. \bar{T} is found by calculating the tunneling probability from the less-doped slab through the heavily doped thin layer ballistically into the metal film and by averaging over the Fermi sphere corresponding to the lower density $\bar{n}_p = 5 \times 10^{19}$ cm⁻³. Listed in Table I are the results for \bar{T} as well as input for its computation:¹⁷ the Schottky barrier height Φ_b and the depletion width w_d . The ballistic approximation in the heavily doped silicon layer is based on mobility data estimates of the mean free path for the electron there to be about 200 Å, i.e., close to the thickness of the layer. If the transport were not ballistic, we would treat the tunneling from the Fermi sea of the heavily doped layer through the space-charge layer. This

TABLE I. Parameters used.

	Cu	Ag	Al
v_{Fm} (10^6 m/s) ^a	1.57	1.39	2.03
τ (10^{-13} s) ^a	2.1	2.0	0.65
ω_b^{-1} (10^{-10} s) ^b	1.4	0.23	7.1
Φ_b (eV) ^c	0.58	0.78	0.72
w_d (Å) ^c	17.4	19.8	19.1
\bar{T}	2.5×10^{-2}	8.9×10^{-3}	9.0×10^{-3}
f ^d	0.013	0.016	0.0077
η ^e	6.9×10^{-3}	4.8×10^{-4}	6.6×10^{-5}
$\eta/(f\bar{T} + \eta)$	0.96	0.77	0.49
Λ (10^{-6} m)	55	8	360
$\omega_b \tau \Lambda (= v_{Fm} \tau / 4)$ [Å]	820	700	330
$\omega_b \tau \Lambda \bar{T}$ (Å)	21	6.2	2.9

^aRef. 16.^bRef. 15.^cRef. 17.^d $f = 6(k_{Fs}/k_{Fm})^2$, $k_{Fs} = 6.3 \times 10^{-2}$ Å⁻¹.^eHarmonic mean of data from Ref. 22.

would change the tunneling probability and, therefore, the scale of the δH versus metal film thickness without otherwise changing the L_m dependence significantly.

The diffusion coefficient D in the thick layer required for Eq. (2) is estimated from mobility data (using six conduction valleys in Si). The bulk limit of the linewidth increase, $\delta H(L_m \rightarrow \infty)$ (Table II, case I, $\epsilon = \bar{T}$),²¹ is approximately 3 times larger than the corresponding experimental plateau values. In Table II, case II, we consider the possibility that at the plateau every tunneling electron may not be spin disoriented before returning to Si. Table I shows that for Cu and Al, when the plateau value is first reached, $L_m/\Lambda \ll \eta$, i.e., spin scattering in the bulk metal is negligible compared to spin scattering at the free metal surface and metal-Si interface. This indicates that the observed plateaus in δH for Cu and Al are not the true bulk limit. Assuming that the free surface dominates the surface spin scattering, we used the experimental values²² of η for the metal surface. In this limit, the first plateau height is given by Eq. (9), independent of the metal thickness. The estimates are shown in Table I. For Al, the calculated values for δH in Table II, case II, are in better agreement with experiment than for case I, but such is not the case for Cu.

The linewidth increase δH is sensitive to the parameters v_{Fs} , D , and the silicon thickness L , whose values are only known approximately. For the dependence of δH on L_m it is better to consider the ratio $\delta H(L_m)/\delta H(\text{plateau})$, which ap-

TABLE II. Plateau values for δH in units of Gauss. For the theoretical estimates we use $v_{Fs} = 1.8 \times 10^5$ m/s and $L = 1$ μm .

Case	$D = 9.5 \times 10^{-4}$ m ² /s			$D = \infty$		
	Cu	Ag	Al	Cu	Ag	Al
I: $\epsilon = \bar{T}$	46	21	22	73	26	26
II: $\epsilon = \bar{T}\eta/(\eta + f\bar{T})$	45		12	70		13
Experiment	12.5	9.1	7.1	12.5	9.1	7.1

proximately corresponds to the values of ϵ . For the metals considered here the criterion $L_m/\Lambda \gg f\bar{T} + \eta$ is apparently not fulfilled for $L_m < 100$ Å (see Table I), and the experimentally observed plateaus are not expected to correspond to the second plateau discussed in Sec. IV B 1. However, Eq. (7) predicts a rapid change in $\epsilon(L_m)$ for thicknesses around $\omega_b \tau \Lambda (\bar{T} + \eta)$ (which is seen from Table I to be less than 25 Å for our metals) from the small- L_m value $\bar{T}(\eta + L_m/\Lambda)/(\bar{T} + \eta)$ to the large- L_m value $\bar{T}(\eta + L_m/\Lambda)/(f\bar{T} + \eta + L_m/\Lambda)$. For Cu, Ag, and Al films the mean free path $\omega_b \tau \Lambda$ ranges from 800 to 300 Å at 77 K. For our samples \bar{T} is found to be of order 0.01 and larger than η . Thus $\omega_b \tau \Lambda (\bar{T} + \eta) \approx \omega_b \tau \Lambda \bar{T}$ corresponds roughly to the metal thickness for which the experimental curve would be expected to rise towards the plateau (see the last row of Table I). Note that $\omega_b \tau \Lambda \bar{T} (= \tau v_{Fm} \bar{T} / 4)$ is the film thickness for which the average time an electron spends in the metal film before returning to the semiconductor equals τ .

For Cu, $\omega_b \tau \Lambda \bar{T}$ is estimated to be 21 Å. Thus, the model with specular reflection off flat surfaces is not in agreement with the rapid onset of the plateau in the experiment. From Eq. (8) and the parameters listed in Table I we also find that a model with diffuse scattering off flat surfaces cannot account for this rapid onset. In the next subsection, we explore the consequences of the island formation at the interface for $L_m < 20$ Å.

For Al and Ag the flat-surface model with specular reflections can account for the thickness dependence observed in the experiment. For Al, flat surfaces with diffuse scattering could be ruled out, while for Ag, where $\Lambda(f\bar{T} + \eta)$ is only ~ 50 Å, the diffuse scattering formula Eq. (8) predicts a rise to a plateau for a value of L_m of the same magnitude as in the experimental curve.

B. The island model

We compare the calculated thickness dependence of δH using the island model Eq. (14) and rough surfaces with the measured data in Fig. 2. The dashed lines are the results of applying this model with $h_0 = 10, 22,$ and 22 Å for Cu, Ag, and Al, respectively, where $\delta H(100 \text{ Å})$ is normalized to the experimental data. Note that the Ag value for h_0 is close to that found in Ref. 20.

While the flat-surface model can also account for the experimental data in Ag and Al, there is additional evidence for the presence of islands in data taken for Al-Cu bilayer samples shown earlier in Fig. 4. The bilayer data suggest in agreement with the pure Al results above, that for initial Al layers thinner than a few tens of angstroms, Al islands partially cover the Si surface. This is also in qualitative agreement with previous studies using Auger electron spectroscopy for Al on cleaved Si(111).²⁵

C. Significance of the theoretical results

The spin disorientation probability involves both charge transport and spin scattering. For charge transport, our theory includes in a simple way tunneling through the Schottky barrier and the momentum scattering in the metal. The sources of spin scatterings include the far metal surface, the metal-

semiconductor interface, and the metal bulk. For flat surfaces the major thickness dependence of the spin disorientation arises from whether the film is thick enough to assure that an electron that tunnels into the metal film suffers a *momentum-scattering* collision before tunneling back into the Si slab. The same effect is also present in the island model, but then this effect is made less transparent by the thickness dependence of the island structure.

While the roughness of the approximations for the transport and spin scattering quantities needed rendered it impossible to assess the accuracy of our calculated results for the increase of CESR linewidth, the error in our estimate of the thickness dependence for smooth and flat surfaces is related to the accuracy of our estimate of the ratio of $\eta + \bar{T}$ to $L_m/v_{Fm}\tau$. Both τ and η come from experimental measurements while the tunneling rate \bar{T} (and v_{Fm}) are calculated. All four quantities should be correct within an order of magnitude. However, the more important point is that the theory together with the measurements provides a distinction between the consequences of the flat interface model and island formation. In this way we establish that the experimental results favor the island model, providing a key understanding of the physical cause of how the balancing of the bulk and interface-surface processes works in an appropriate interface environment.

VI. CONCLUSIONS

By heavily doping Si in the Schottky barrier with a metal, we have shown that it is possible to measure an increase in the CESR linewidth for the Si conduction electrons. This is interpreted as the Si electrons tunneling into the metal, which provides a tool for probing the electronic properties across the semiconductor-metal interface.

By comparing the experimental data with our model calculations we find that for Ag and Al the data can be explained both by flat-surface and island models. In contrast, for Cu and Al-Cu bilayers, the data unambiguously favor the rough-surface island model.

While our theory is thus able to account for the experimental observations, further confirmation of the island model requires, in addition to the CESR experiments, separate characterization measurements of the surface structure. Modest modification will allow the measurement of magnetoresistance under weak localization conditions for an independent quantitative determination of the spin relaxation by atoms deposited on the free surface of a thin (~ 100 Å) metal film.²⁴

A practical, and most important, extension of this CESR technique would be to utilize selected alkalis (Na, K, and Rb) for the metal depositions. These metals can have extremely long spin relaxation times ($T_2 \sim 10^{-7}$ sec) at low temperatures, which would allow meaningful measurements with much thicker films, and also provide direct separation of spin relaxation at the interface and that at the free metal surface. The long T_2 also allows one to observe both the Si:P and alkali-metal CESR lines, and the range of g values available can then be exploited to determine the tunneling probabilities by studies of the motional narrowing.¹⁰

ACKNOWLEDGMENTS

We thank Patrice Strehle for her help in preparing the phosphorus-doped Si wafers. The experimental work (J.M.A., D.C.V., and S.S.) was supported by ONR Grants No. N00014-87-K-0338 and No. N00014-90-J-1165 and NSF Grant No. DMR 93-02913. G.T.E. is supported by the Norwegian Research Council. G.T.E. and L.J.S. are supported in part by NSF Grants No. DMR 91-17298 and No. DMR 94-21966.

*Present address: Institutt for tekniske fag, Norges Landbrukshøgskole, Postboks 5065, 1432 Ås, Norge.

¹Preliminary CESR studies of n -doped silicon covered with metal films have been reported in D.C. Vier and S. Schultz, in *Proceedings of the 18th International Conference on the Physics of Semiconductors, Stockholm*, edited by Olof Engström (Chalmers, Göteborg, 1986), Vol. 1, p. 243; D.C. Vier, S. Schultz, M.G. Wu, and M.B. Maple, *J. Vac. Sci. Technol. B* **5**, 985 (1987).

²S. Schultz, in *Measurements of Physical Properties*, edited by R.F. Bunshah (Wiley, New York, 1972), Vol. 6, P. 1, p. 337.

³R.H. Taylor, *Adv. Phys.* **24**, 681 (1975).

⁴R.H. Taylor, *Magnetic Ions in Metals: A Review of Their Study by Electron Spin Resonance* (Halsted Press, New York, 1977).

⁵G. Feher and A.F. Kip, *Phys. Rev.* **98**, 337 (1955).

⁶L.D. Bell and W.J. Kaiser, *Phys. Rev. Lett.* **61**, 2368 (1988).

⁷J.J. Baumberg, S.A. Crooker, D.D. Awschalom, N. Samarth, H. Luo, and J.K. Furdyna, *Phys. Rev. B* **50**, 7689 (1994).

⁸L.J. Sham, *Acta Phys. Pol. A* **87**, 7 (1995).

⁹L.D. Flesner, D.R. Fredkin, and S. Schultz, *Solid State Commun.* **18**, 207 (1976).

¹⁰D.C. Vier, D.W. Tolleth, and S. Schultz, *Phys. Rev. B* **29**, 88 (1984).

¹¹D.M. Eigler and S. Schultz, *Phys. Rev. Lett.* **54**, 1185 (1985).

¹²H. Flaum, Ph.D. thesis, University of California, San Diego, 1991.

¹³J.M. Anderberg, Ph.D. thesis, University of California, San Diego, 1993.

¹⁴M.R. Menard and M.B. Walker, *Can. J. Phys.* **52**, 61 (1974).

¹⁵D. Lubzens, Ph.D. thesis, University of California, San Diego, 1975. For Cu and Ag we have extrapolated low-temperature results to 77 K.

¹⁶N.W. Ashcroft and N.D. Mermin, *Solid State Physics* (Saunders College, Philadelphia, 1976).

¹⁷S.M. Sze, *Physics of Semiconductor Devices*, 2nd ed. (Wiley, New York, 1981).

¹⁸G.T. Einevoll and L.J. Sham, *Phys. Rev. B* **49**, 10 533 (1994).

¹⁹Yan-Ten Lu and L.J. Sham (unpublished).

²⁰E.J. van Loenen *et al.*, *Surf. Sci.* **137**, 1 (1984).

²¹G.W. Graham and R.H. Silsbee, *Phys. Rev. B* **22**, 4184 (1980).

²²S. Sako, *J. Phys. Soc. Jpn.* **60**, 265 (1991).

²³P. Chen, D. Bolmont, and C.A. Sebenne, *J. Phys. C* **17**, 4897 (1984).

²⁴A. Starr, S. Schultz, and A. Nishida (unpublished).